CONFERENCE PRE-PRINT

INVESTIGATION OF FILAMENT DYNAMICS USING HIGH-SPEED VIDEO SHOOTING IN THE GLOBUS-M2 TOKAMAK

V.M. TIMOKHIN
Peter the Great St. Petersburg Polytechnic University
Saint-Petersburg, Russian Federation
Email: v.timokhin@spbstu.ru

[1,2]M.K. BUTS, [1]V.YU. SERGEEV, [2]A.N. NOVOKHATSKY, [1]D.D. KOROBKO and [2]GLOBUS-M2 TEAM
[1]Peter the Great St. Petersburg Polytechnic University
Saint-Petersburg, Russian Federation
[2]Ioffe Institute
Saint-Petersburg, Russian Federation

Abstract

The aim of this study was to develop and integrate high-speed cameras set into the Globus-M2 tokamak diagnostic system, which was successfully done. Several series of experiments were conducted using high-speed video shooting of the Globus-M2 tokamak's peripheral plasma across a wide range of discharge parameters and shooting modes. A software package was developed to automate the processing of the results obtained. Processes occurring during the growth of edge localized instability modes in Globus-M2 tokamak's peripheral plasma were registered in the visible spectral range. The conditions for the formation of edge localized modes filaments were investigated. Filament's key parameters were estimated, including transverse dimensions, velocity, and the total number of filaments at the low field side.

1. INTRODUCTION

The study of edge localized modes (ELM) and associated plasma filaments is a crucial goal in the context of limiting the maximum heat fluxes on the first wall components of tokamaks [1]. It can also contribute to understanding the mechanisms of heat and particle transport in the edge plasma. Filaments detection is carried out on many tokamaks. The primary diagnostics used for this purpose are Langmuir probes [2] and Doppler backscattering (DBS) [3]. However, these diagnostics have low spatial resolution. Detailed investigations of both a temporal evolution and a spatial structure of filaments can be achieved using fast photography techniques. Studies of filaments using fast camera have been conducted on the MAST tokamak [4, 5]. This has provided information on the number, spatial structure, mode numbers, velocities, and dimensions of filaments, demonstrating the highly informative content of this diagnostic technique. This paper presents the first results of high-speed imaging of ELM filaments on a Globus-M2 tokamak and performs their preliminary analysis.

2. DESCRIPTION OF THE DIAGNOSTIC SYSTEM

A new high-speed camera diagnostic system has been developed for the Globus-M2 spherical tokamak. The system includes three high-speed cameras: Phantom Miro M110, Revealer X213, Optronis CR3000X2 (see the main technical specifications in Table 1), the multichannel clock generator Stanford Research Systems DG645 for synchronizing the cameras, and a set of lenses and filters. The set of the lenses includes the following models: Tamron 18-200mm F/3.5-6.3, Nikon 18-55mm F/3.5-6.5, Laowa 100mm F/2.8-5.6, Zenithar 8mm F/3.5-22 (fisheye). The large range of focal lengths of the lenses allows one to adjust the field of view and spatial resolution within wide limits.

A photo of the main diagnostic elements installed on the tokamak is shown in Figure 1. The numbers indicate the following diagnostic elements: 1– Revealer camera on a solid tripod; 2 – Optronis camera on a tripod with a crossbar; 3 – Phantom camera with the polychromator [6] on adjustment mount to tokamak. The imaging is performed from the equatorial port of the tokamak, covering a wide field of view of the Globus-M2 vacuum chamber. This includes both the peripheral regions, as well as the central region of the plasma column and both the upper and lower divertor regions. This is made possible by adjusting the position of the cameras relative to the port over a wide range. The cameras' viewing areas are shown in Figure 2 (Green sector). When the temporal or spatial resolution of high-speed video is increased, the field of view has to be narrowed (see Figure 2, Blue and Red sectors). In addition, a system for collecting, storing and processing diagnostic data has been developed. The

novel use of multiple cameras allows for simultaneous wide-view plasma imaging and high-speed measurements with a reduced camera resolution of the same plasma region.

TABLE 1. FAST CAMERAS BASIC PARAMETERS

	Optronis CR3000X2	Phantom Miro M110	Revealer X213
Sensor type		CMOS	
Pixel size, μm	8	20	14.6
Sensor resolution, pxs	1696x1710	1280x800	1280x1024
Dynamic range, bits	8	12	8
Max. frame rate at full resolution, fps	543	1630	13 600
Max. frame rate at reduced resolution, fps (frame size, pxs)	142 857 (8x8)	400 200 (64x8)	1 000 000 (1280x8)
Minimal exposure time, μs	2		0.1

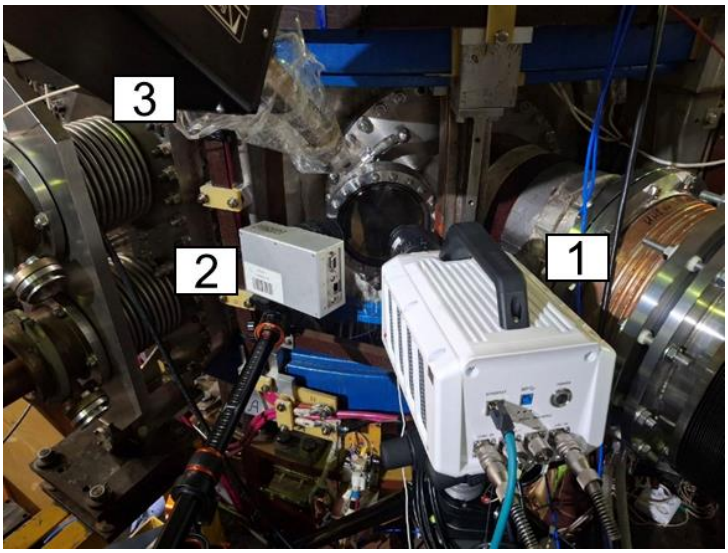

FIG. 1. Photo of the fast cameras near the equatorial port with a window of the Globus-M2 tokamak. 1 - Revealer X213, 2 - Optronis CR3000X2, 3 - Phantom Miro M110 with the polychromator [6].

3. IMAGE PROCESSING

Several software packages were developed and utilized to process and analyze the videos obtained. First of all, the modern original program with a friendly graphical user interface Fast Camera Viewer (FCV) [7] was developed. This program allows for convenient frame-by-frame video display and synchronization with data from other tokamak diagnostics, as well as frame processing and spatial measurements.

To accurately measure the characteristics of the filaments, an original algorithm has been developed to increase the contrast of the filamentous images. The characteristic poloidal velocities of filaments in the Globus-M2 tokamak range from 5 to 15 km/s was measured [8]. It requires an exposure time of 1-10 microseconds to capture them reliably. At the same time, the intensity of the filaments is usually only slightly higher than the background plasma emission. To isolate rapid changes in brightness against the relatively slow-varying glow of the main plasma, methods of "subtracting" the static background from the image are applied. The classical algorithm [9] involves median and Gaussian filtering, calculating the background by simple averaging of several adjacent frames, and subtracting this background from the image. In the proposed method, median and bilateral filtering are used, and background subtraction is performed based on an original algorithm using the formula:

$$F^i_{\alpha\beta} = A^i_{\alpha\beta} - \left(\frac{1}{N} \sum_{k=i-\frac{N}{2},\, k\neq i}^{i+\frac{N}{2}} A^k_{\alpha\beta} - \frac{1}{N(N-1)} \sum_{m=i-\frac{N}{2},\, m\neq i}^{i+\frac{N}{2}} \sum_{k=i-\frac{N}{2},\, k\neq m,i}^{i+\frac{N}{2}} (A^k_{\alpha\beta} - A^m_{\alpha\beta}) \right).$$

Here A, F are the luminosity of the image matrix ($\alpha\beta$) pixel before and after background subtraction correspondingly, the superscript is the image serial number, the subscripts are the pixel coordinates in the image, N is the number of frames used to calculate the background.

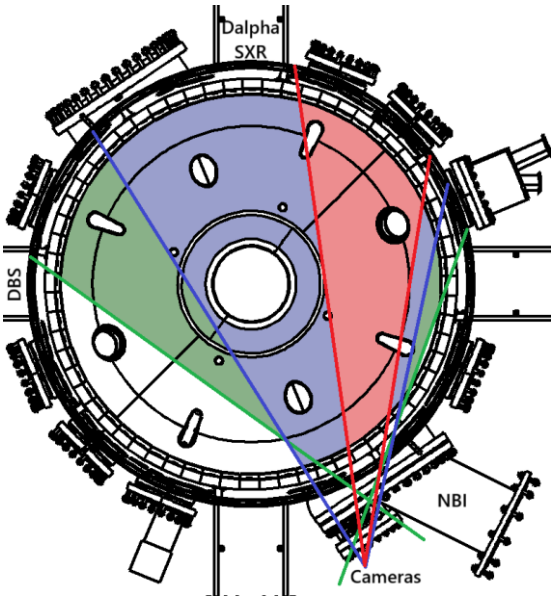

FIG. 2. Cameras' fields of view. Green – the entire observable area. Blue – field of view in shot 44044 (Figure 3, 4, 5) at low frame rate. Red – field of view in shot 44297 (Figure 6) at high frame rate.

This algorithm offers a way to take into account the additional brightness increase of the classical background (the first two terms of the formula) that occurs due to averaging many filaments across frames. The additional third term of the formula represents the average luminance of the filaments across the frames. This approach has allowed for a 2.5-fold reduction in background subtraction errors on synthetic filament images compared to the classical algorithm. This significantly simplifies image interpretation due to fewer distortions and higher contrast.

Spatial calibration of the fast cameras' field of view was performed using the CalCam code [10]. This code calculates the camera's position and viewing direction, field of view, and lens distortion using a point-fitting method comparing 3D CAD model of the tokamak and internal elements of the vacuum chamber. As a result, it was possible to determine the position and dimensions of recorded objects in the tokamak plasma with an accuracy of ~1 mm.

Magnetic field lines were traced using the PLEQUE [11] and FreeGS [12] codes based on magnetic equilibria calculated using the pyGSS [13], FreeGS, and MCC [14] codes. The field line was superimposed on the image using the CalCam code and the calibration procedure mentioned above.

As a result, it was shown that the observed filamentary structures coincide in direction with the magnetic field lines lying nearby the separatrix with good accuracy (1-2 cm). No deviations at large distances from the separatrix were observed. An example of the calculation results is shown in Figure 3, where three magnetic field lines (in different colors) are superimposed on the processed contrast image of the filamentary structures. Filaments were extracted, intensified and overexposed on the raw image. The magnetic field lines illuminated by filaments lie on the separatrix in the area of the outer wall of the tokamak vessel, and they also correspond to them near the inductor column and in the divertor area. The camera was positioned horizontally on the midplane. The tokamak's central column is clear visible on the left. The tokamak wall is visible on the right. The viewing area on the right

is limited by the flange edge. Technical information about the discharge and imaging mode is provided in the lower right corner of the figure.

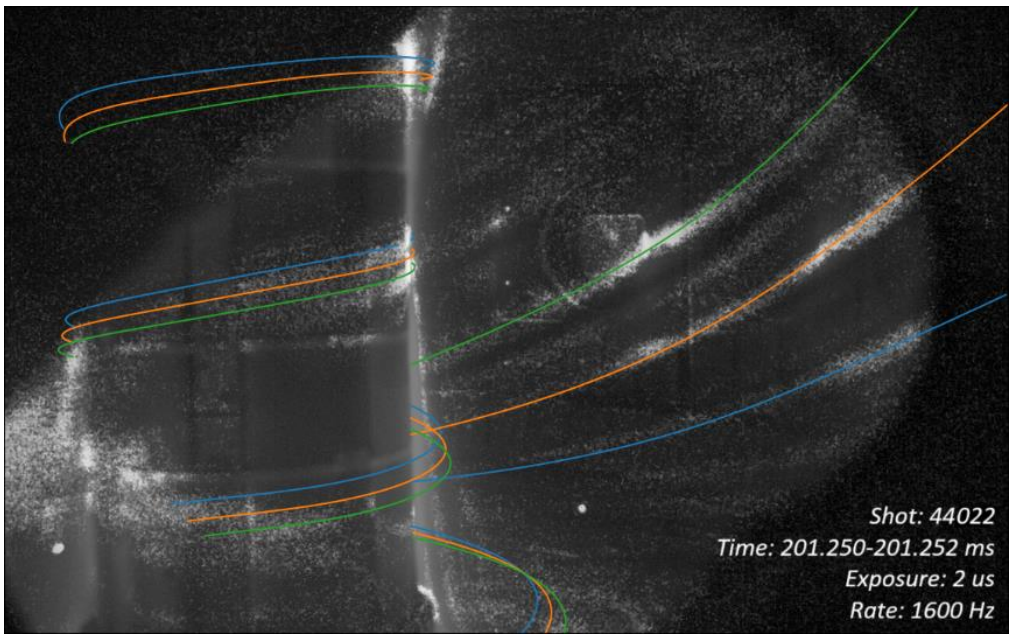

FIG. 3. An example of projecting the magnetic field lines onto an experimental image with filaments.

4. EXPERIMENT RESULTS

By analyzing high-speed videos in various tokamak operating modes (approximately 50 discharges), it was possible to identify filamentary structures elongated in the magnetic field direction, located primarily on the low-field side nearby separatrix. The presence, intensity, and number of the filaments have not yet been linked to the presence or absence of both a transport barrier at the plasma edge (L or H-mode) and an additional heating (OH or OH+NBI heated regimes).

An example of an image of filamentary structures is shown in Figure 4 for the 44044 discharge, the main plasma parameters are as follows: toroidal magnetic field of 0.7 T, plasma current of 300 kA, central electron density of $5.5 \cdot 10^{19}$ m^{-3}, NBI heating power of 0.8 MW. The left part of the figure shows instantaneous images of the fast Phantom camera at the full resolution of the matrix (1280x800 pxs), the approximate viewing sector is shown in Blue in Figure 2, exposure time of 2 μs, frame rate of 1600 Hz. The upper part shows a raw image, the lower part – background subtracted image processed by procedure described in the previous section. The right part shows temporal evolutions of measured signals of monitoring diagnostics that can be used to identify the presence of ELM in the plasma: the Dα emission signal in the lower divertor (plasma with a lower x-point), the soft X-ray signal SXR along the central chord with a 50 μm thick beryllium filter and the MHD loop signal. The bottom graph represents the averaged intensity of the image frame calculated separately for the central column region (left half of the image, blue line on the figure) and for the region of the outer vessel wall, where filamentary structures are predominantly observed (right half of the image, orange line on the figure). The camera exposure time was selected to coincide with the moment of the Dα signal burst, accompanied by an internal crush of the plasma characterized by a sharp drop in the SXR signal and a burst in the MHD signal. Approximately 10 filamentary structures can be observed on the outer side of the plasma, particularly noticeable in the processed image (bottom left image of the figure). Also noteworthy is the intense illumination of the central column, the lower divertor region, and the flanges edges on the low-field side.

Figure 5 shows the same discharge, with the exposure time selected 1.2 ms apart from that shown in Figure 4. This corresponds to the moment between Dα signal bursts. All signals and designations are the same as in Figure 4. At this moment filamentary structures on the low-field side are also clearly visible. Their number and size correspond closely to those observed during the Dα burst. A significant difference from the image shown in Figure 4 is the lack of illumination of the inductor column and the lower divertor region. Areas of increased radiation intensity are also visible on the flanges area on the low-field side.

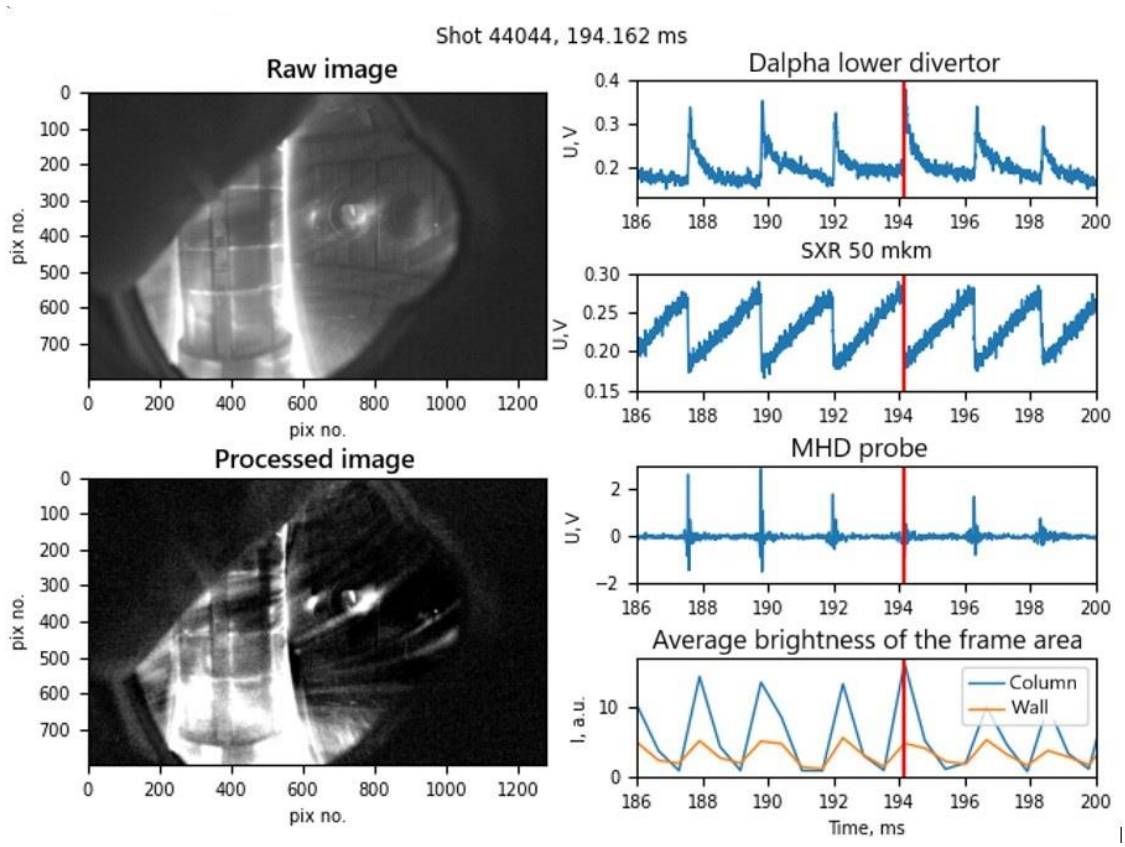

FIG. 4. An example of a frame with an instant image of filamentous structures at the moment of a Dα signal flash.

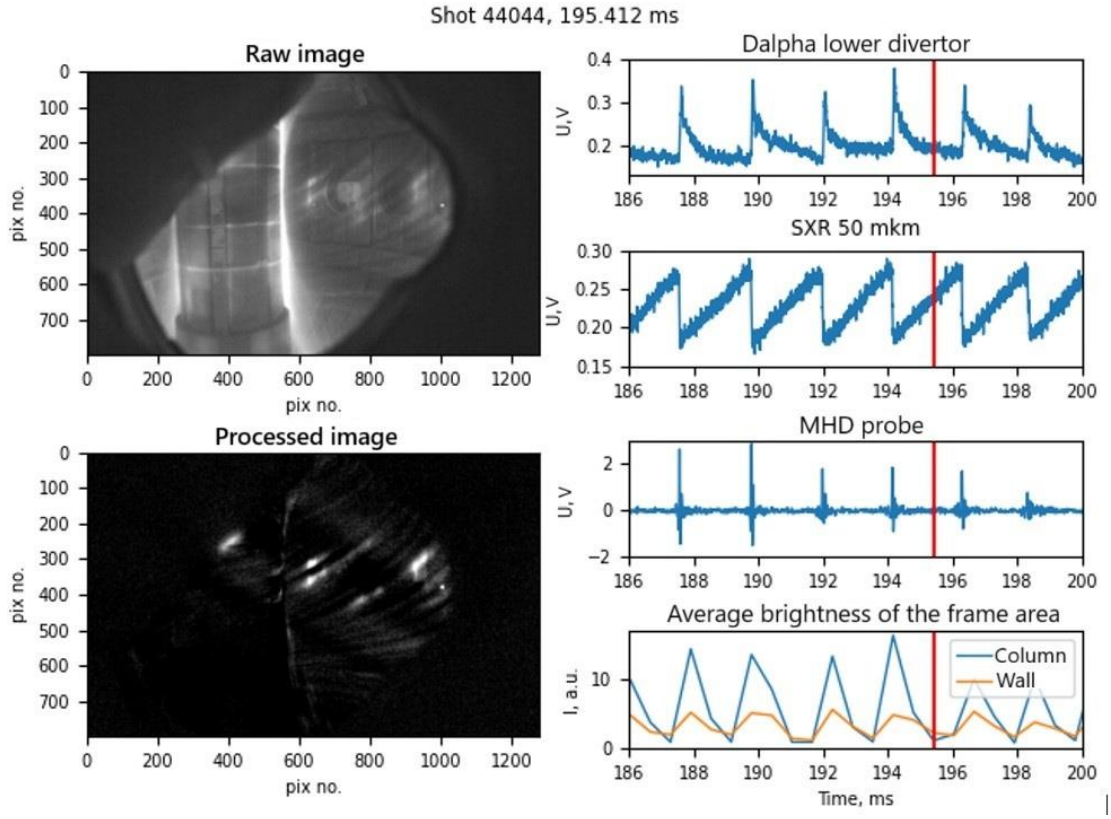

FIG. 5. An example of a frame with an instant image of filamentous structures without a Dα signal flash.

Thus, comparison of snapshots in Figures 4 and 5 allows us to conclude that the main source of the signal on the Dα detectors during the ELM event is the central column and the divertor region, but not the filamentary structures. This is a fundamental difference from the phenomena observed at the MAST tokamak [4], where the main source of the Dα signal during ELM are filamentary structures mainly. This may be due to differences in the vacuum vessel design. At the MAST tokamak, the plasma is located at a significantly greater distance from the walls of the vacuum vessel than at Globus-M2. This may also be due to the fact that at the Globus-M2 tokamak in the described regime, ELM events caused by internal reconnection events (sawtooth oscillations) are predominantly observed [15].

A similar situation is seen analysing discharges without additional NBI heating, where filamentary structures are also present regardless of the sawtooth oscillation phase, and the main sources of radiation during Dα bursts are the central column and divertor region. The total number of filaments at the low field side and their transverse dimensions also remain significantly unchanged. The only difference is a slight decrease in the overall frame illumination intensity and, correspondingly, lower contrast of the observed filamentary structures, which is likely due to the lower energy content of the plasma in the absence of NBI power.

The above reasoning is based on an analysis of images with short (~ several microseconds) exposures at the full resolution of the matrix of fast cameras. The design of these cameras allows for a significant increase in the frame rate by reducing the matrix readout area. This feature made it possible to estimate the poloidal velocity of the filamentary structures observed on the low-field side of the tokamak near the separatrix. This estimation is illustrated in Figure 6 for discharge 44297, the main plasma parameters being as follows: toroidal magnetic field of 0.7 T, plasma current of 210 kA, central electron density of $5.6 \cdot 10^{19}$ m^{-3}, and NBI heating power of 0.8 MW. Filming was conducted with a Phantom camera with an exposure time of 5 mks, a frame rate of 77 kHz, and a frame resolution of 128x128 pixels. Figure 6 shows a reference image in the absence of plasma, demonstrating the camera's field of view (see Red sector in Figure 2), providing a spatial reference based on the tokamak vessel's elements size. Five consecutive frames of shot 44297 are shown, revealing a filamentary structure shifting from top to bottom across the image. The average offset of the filament from frame to frame is ~4 cm. Calculations give an estimated filament velocity of ~5.5 km/s based on its shift on the midplane in a direction perpendicular to the magnetic field lines. The transverse size of the filament (in the direction perpendicular to the magnetic field) is ~3 cm. This size estimate takes into account that the filament in the image is broadened due to its movement during the exposure time. The scale is calibrated based on the sizes of the carbon tiles shown in red arrows in Figure 6.

Similarly, using the Revealer camera, the poloidal velocity of the filaments at the bottom part of the plasma column, near the divertor, was estimated. This gave a slightly lower filament velocity of ~3 km/s, approaching the transverse size of ~3 cm.

Hence wide-view images allow for the determination of the toroidal number of filaments, which is approximately 10–25. Imaging with lower camera resolution and higher frame rates enabled the recording of filament dynamics and the determination of their poloidal velocities (~3–15 km/s) and transversal sizes (~2–3 cm). These results correspond reasonable to theoretical predictions and the DBS measurements [8].

5. CONCLUSIONS AND DIAGNOSTIC DEVELOPMENT PLANS

To sum it up, a diagnostic complex for high-speed plasma imaging and a set of programs for video processing and data comparison with other diagnostics of the Globus-M2 tokamak were created. A series of measurements of the peripheral plasma of the Globus-M2 tokamak was performed using high-speed cameras in the visible light range. It was possible to register filamentary structures elongated in the direction of the magnetic field, moving downwards from the equatorial plane to the divertor direction. Typical filament parameters were measured: size 2-3 cm, velocity ~3-15 km/s, full number 10-25. These parameters correspond to theoretical predictions and data from other diagnostics. Based on the angle of inclination of the filaments, their localization near the separatrix is shown. A correlation between the number and brightness of filaments and sawtooth oscillations and Dα signal bursts is not always observed. A strong correlation between the filament intensity and the phase of the sawtooth is not found. The main source of signal on the Dα detectors during the ELM flash on Globus-M2 is the central column, the divertor region, and the outer wall of the chamber, but not the filamentary structures. Given the measured filament parameters, reliable detection requires imaging with exposure times shorter than 10 mks.

Future plans for diagnostic development include imaging filaments in the near field (just in front of the observation port) as well at central column region to attempt to elucidate their internal structure. Simultaneous imaging with

two cameras, a "fast" camera and a "survey" camera, is also planned, using a single perspective, as well as multi-angle imaging of filamentary structures. Another important objective is the use of narrow-band interference filters to verify the spectral properties of filaments.

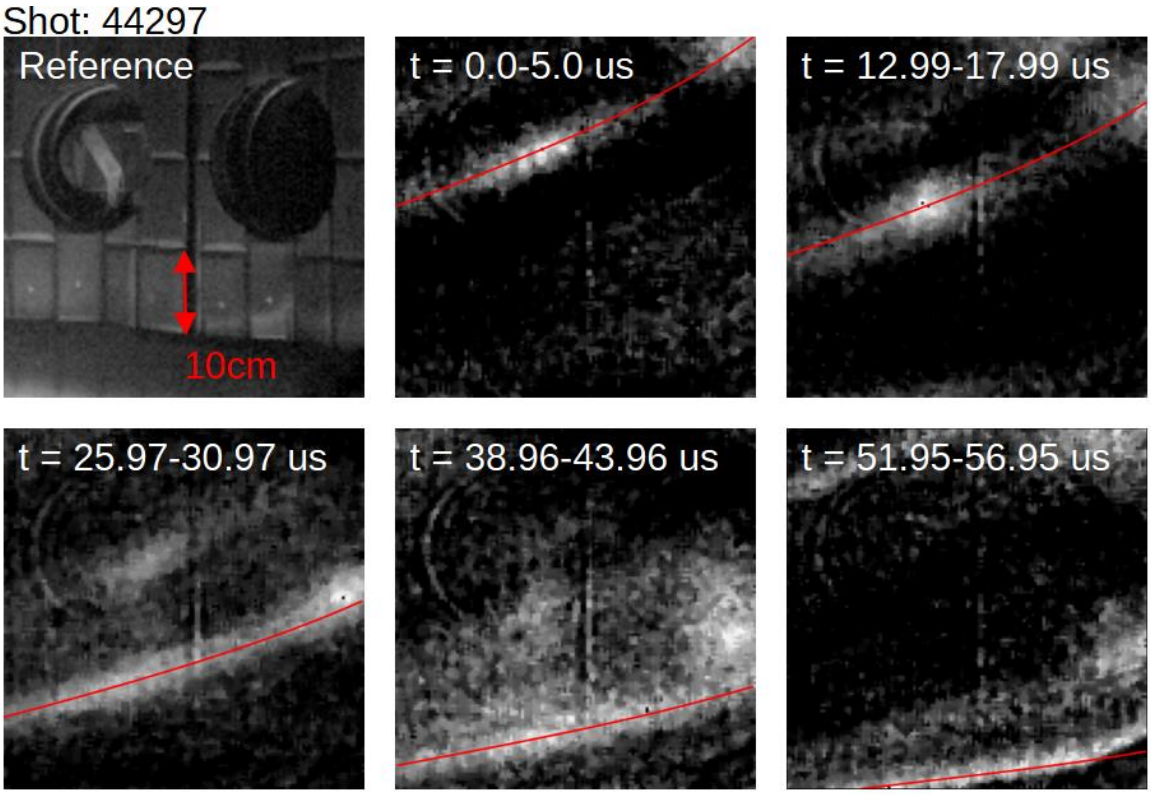

FIG. 6. An example of observing the dynamics of filament motion and estimating its poloidal velocity.

ACKNOWLEDGEMENTS

This work was supported by the Ministry of Science and Higher Education of the Russian Federation as part of the state assignment in the field of science under Project № FSEG-2024-0005. The research utilized the Federal Center for Collective Use "Materials Science and Diagnostics in Advanced Technologies" at the A.F. Ioffe Physical-Technical Institute, which includes the Unique Scientific Facility "Globus-M Spherical Tokamak". The development of high-speed camera diagnostics was supported by Rosatom State Corporation and the Ministry of Education and Science of Russia within the framework of Federal Project 3 (FP3), project № FSEG-2025-0002 “Development of principles and systems for control and diagnostics of tokamak plasma using substance injection”.

REFERENCES

[1] FUNDAMENSKI W. et al., ELM-wall interaction on JET and ITER, Journal of Nuclear Materials 363–365 (2007) 319–324

[2] BENCZE A. et al., On the statistics of ELM filaments measured by fast low field side wall Langmuir probes on TCV, 34th EPS Conference on Plasma Phys. Warsaw, 2-6 July 2007 ECA Vol.31F, P-2.026 (2007)

[3] PONOMARENKO A. et al., The investigation of edge-localized modes on the Globus-M2 tokamak using Doppler backscattering, Nucl. Fusion 64 022001 (2024)

[4] KIRK, A. et al., Spatial and Temporal Structure of Edge-Localized Modes, 2004 Phys. Rev. Letters, vol. 92, Issue 24

[5] FARLEY T. et.al., Filament identification in wide-angle high speed imaging of the mega amp spherical tokamak. Rev. Sci. Instrum. (2019); 90 (9)

[6] TIMOKHIN V.M. et al., Spectroscopic Diagnostic of the Peripheral Plasma in the Globus-M2 Tokamak with the Injection of Neutral Helium, JETP Letters, Vol. 116, No. 5, (2022) 300–306
[7] BUTS M.K., Fast Camera Viewer package, https://github.com/MikhailButs/Fast-Camera-Viewer
[8] YASHIN A.Y. et al., Determination of filament parameters on the spherical tokamak Globus-M2 using Doppler backscattering, Technical Physics Letters, Vol. 49, No. 7 (2023)
[9] FARLEY T. et al., Analysis of Scrape-Off Layer Filament Properties Using Visible Camera Data, 3rd IAEA Technical Meeting on Fusion Data Processing, Validation and Analysis (2019)
[10] SILBURN S., et al., Calcam Python package, DOI: 10.5281/zenodo.14041548
[11] KRIPNER L., et al., PLEQUE Python module, https://github.com/kripnerl/pleque
[12] DUDSON B., et al., FreeGS Python module, https://github.com/freegs-plasma/freegs
[13] KISELEV E.O. et al., Free-Boundary Plasma Equilibrium Computation in Spherical Globus-M2 Tokamak by Means of the pyGSS Code. Plasma Phys. Rep. 49, (2023) 1560–1577
[14] SAKHAROV N.V. et al., Reconstruction of equilibrium magnetic configurations in the Globus-M spherical tokamak. Plasma Phys. Rep. 41, (2015) 997–1001
[15] BULANIN V.V. et al., The model of synchronization between internal reconnections and edge-localized modes, Plasma Physics and Controlled Fusion, Volume 63, Issue 12, id.122001, 7 pp. (2021)